# A Novel Design of Hybrid Energy Storage System for Electric Vehicles

*Xiangyang Xia*[1,2]*, *Xinxin Zhao*[1], *Heqing Zeng*[1], *and Xiaoyong Zeng*[1]

(1. College of Electrical and Information Engineering, Changsha University of Science and Technology, Changsha 410004, China;
2. Engineering Research Center of Power Grid Safety Monitoring & Control Technology, Ministry of Education, Changsha University of Science and Technology, Changsha 410004, China)

**Abstract:** In order to provide long distance endurance and ensure the minimization of a cost function for electric vehicles, a new hybrid energy storage system for electric vehicle is designed in this paper. For the hybrid energy storage system, the paper proposes an optimal control algorithm designed using a Li-ion battery power dynamic limitation rule-based control based on the SOC of the super-capacitor. At the same time, the magnetic integration technology adding a second-order Bessel low-pass filter is introduced to DC-DC converters of electric vehicles. As a result, the size of battery is reduced, and the power quality of the hybrid energy storage system is optimized. Finally, the effectiveness of the proposed method is validated by simulation and experiment.

**Keywords:** Hybrid energy storage system, integrated magnetic structure, electric vehicles, DC-DC converter, power dynamic limitation.

## 1 Introduction

Due to the pollution caused by fossil fuel, new energy sources have been continuously developed[1-2]. Nowadays, embedded energy storage systems in current generation electric vehicles are mostly based on the Li-ion batteries which, with high energy density, can provide long distance endurance for electric vehicles. While compared to the super capacitor, the response of Li-ion batteries is slower than that of super capacitors[3-4]. Therefore, in order to make electric vehicles comparable to fuel vehicles with regards to fast transient acceleration, energy, and long-distance endurance, a hybrid energy storage system(HESS) consisting of Li-ion batteries and super-capacitors is applied to electric vehicles[5]. For the development of electric vehicles, optimizing the energy storage device is critical, and it is necessary to consider increasing the capacity of the battery, while reducing the size and weight of the battery to increase the charging rate[6-8].

DC-DC converters which play an important role in hybrid energy storage system have been developed rapidly over the years. Through a series of innovations, a variety of DC-DC converters are proposed. A new zero Voltage Switch (ZVS) bidirectional DC-DC converter is proposed in [9], which has good controllability to improve conversion efficiency, but is not suitable for electric vehicles due to the complex control and higher cost. It has been shown an isolated bi-directional DC-DC converter[10] with complex structure is able to convert a large power transmission. A new zero-ripple switching DC-to-DC converter with the integrated magnetic technologies is first proposed in [11-12] by S.Cuk, and the application is very successful. Isolated interleaved DC/DC converter[13] introduces the concept of three-winding coupled inductors, but it is more suitable for power transmission.

It is very important for hybrid energy storage systems to select a suitable energy management strategy. Energy management strategies have been extensively reported in literature in the recent years, including neural networks, fuzzy logic, state machine control, frequency decoupling method, on/off-line optimal strategies, dynamic programming (DP) and limitation of battery power[14-17]. The main objective of the optimal control strategies is to ensure a continuous supply by the minimization of a cost function. These strategies can be divided into off-line global optimization and on-line local optimization. For off-line global optimization, it is necessary to acquire the best power distribution between different sources. At the same time, for on-line local optimization, accurate predication driving conditions is necessary[18-20].

In this work, a new integrated magnetic structure of DC-DC converter is proposed and applied on hybrid energy storage system for electric vehicles. The proposed DC-DC converter gives the specific topology and operating modes, as well as Li-ion battery and super capacitor control. With regards to energy management strategy, the paper proposes a optimization control algorithm designed using a Li-ion battery power dynamic limitation rule-based control based on the state of charge(SOC) of the super-capacitor. In order to improve the life and reduce the size of hybrid energy storage system, the paper uses a hybrid algorithm based on particle swarm optimization and Nelder-Mead simplex approach to optimize the control parameters. Finally, the simulation and experimental analysis verify the hybrid energy storage system performance.

## 2 Topology of hybrid energy storage system

Fig.1 is a proposed hybrid energy storage system

* Corresponding Author, E-mail:307351045@qq.com.
Supported by National Natural Science Foundation of China (Grant: 51307009).

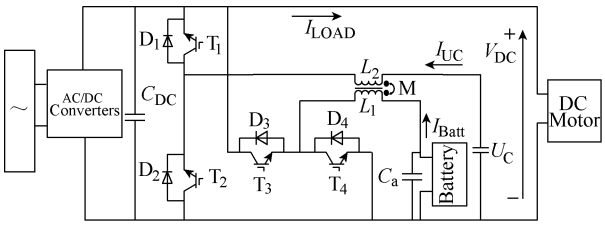


Fig.1 Topology of the hybrid energy storage system

composed of DC/DC converter, super capacitors and the Li-ion battery. DC/DC converters consist of four IGBT switches $T_1$~$T_4$ and its corresponding diode (added battery) tube $D_1$~$D_4$, and an integrated magnetic structure——self inductance $L_1$、$L_2$ and mutual inductance M, which share a core inductors. The battery pack provides power to the smooth DC motor. The super capacitor deals with the instantaneous state of peak power supply. The power management system of electric vehicles determines the electrical energy flow according to the load demand.

The converter has five main operating modes (mode due to the additional battery pack change). Table 1 shows the specific operation mode of hybrid energy storage system corresponding energy flows and operating mode DC-DC converter.

## 3 Design of the DC/DC converter with integrated magnetic structure

Magnetic elements such as inductors, are the main components of energy conversion, filtering, electrical isolation and energy storage. The size of the magnetic element is a major factor in determining the size and weight of the converter.

To achieve the integration of magnetic elements, an E-type magnetic core is used in this paper. Herein, a coupling inductance ($L_1$ and $L_2$) is used. As shown in Fig.2, $L_2$ as the output filter inductor, $L_1$ as the external inductance, and $C_a$ as additional capacitance. In the steady state , the voltage of $C_a$ is equal to the output voltage of $L_2$ and $L_1$ without regard to the capacitor voltage ripple. The DC/DC converter of Fig.1 consists of 4 IGBT switches ($T_1$~$T_4$) and 4 diodes ($D_1$~$D_4$). As a boost converter, there are two operational modes (consisting of $L_1$, $T_4$, $D_4$ or $L_2$, $T_2$, $D_1$); and as a buck converter, there also are three operational modes (consisting of $L_1$, $T_3$, $D_4$ or $L_2$, $T_1$, $D_2$).

**Table 1 The operation mode of hybrid energy storage system**

| Working mode | Power source | Power flow | Operation mode |
|---|---|---|---|
| Parking charging mode | AC power | Battery and super capacitor | Buck |
| Constant speed mode | Battery | DC | Boost |
| Acceleration mode | Super capacitor | DC motor | Boost |
| Braking mode | Braking energy | Battery and super capacitor | Buck |
| Super-capacitor charging mode | Battery | Super capacitors and DC motors | Boost or buck |

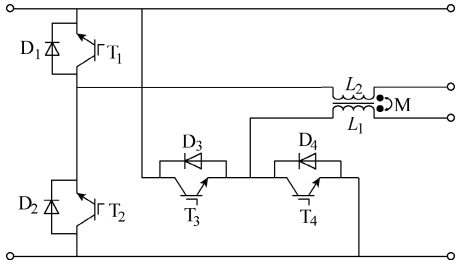


Fig.2 Topology of DC/DC converter with integrated magnetic structure

It can be seen from Table 2, a comparison of two structures of DC/DC converter is illustrates that the volume and weight of the DC/DC converter with integrated magnetic structure are reduced. In the electric vehicle, the application of the DC/DC converter with integrated magnetic structure can reduce the overall size and weight of the energy storage system. Moreover, integrated magnetic structure can reduce the output current ripple. In section 4, the effectiveness of the integrated magnetic structure is validated by simulation and experiment.

## 4 Control strategy of hybrid energy storage system

### 4.1 Super capacitor

A cascade voltage and current controller is selected to provide a stable load voltage. When the DC side voltage has a significant increase during braking, Super-capacitors can make a more rapid response and recycle the braking energy. Fig.3 is the control block diagram of the super capacitor controller.

Where $V_{dc}$ and $V_{dc\text{-}sen}$ are respectively the actual voltage and rated voltage of DC motor; $i^*_{UC}$ and $i^*_{UC-sen}$ are respectively the per unit of super-capacitor actual current and rated current; $f_s$ is the switching frequency; $G_{1,2}$ are the switching signal of $T_1$ and $T_2$.

In boost mode, the duty cycle of the inductor current transfer function can be expressed as:

$$\frac{I_{L2(s)}}{D_{(s)}}=\frac{V_{dc}R_{Load}C_{dc}s+2V_{dc}}{R_{Load}L_2C_{dc}s^2+L_2s+R_{Load}(1-D)^2} \quad (1)$$

$I_{L2(s)}$ is the reference current of $L_2$, $V_{dc}$ is the DC motor voltage, $C_{dc}$ is the capacitor DC motor, $D$ is the duty cycle. In the frequency range, the relationship

**Table2 Comparison of two structures of DC/DC converter**

| Feature | Discrete inductors structure/cm$^2$ | Integrated magnetic structure/cm$^2$ | Effect(%) |
|---|---|---|---|
| Surface area | 79.15 | 60 | −24.20 |
| Core volume | 104.19 | 79.60 | −23.60 |
| Core weight/kg | 0.31 | 0.23 | −25.80 |
| Wire weight/kg | 0.21 | 0.21 | −0 |

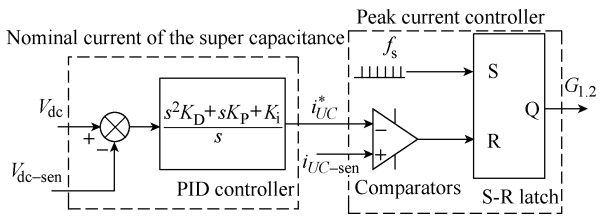


Fig.3 Block diagram of the super-capacitor voltage and current controller

between the inductor current and the DC-side voltage is represented by the following equation ;

$$\frac{V_{\mathrm{dc}}(s)}{I_{L2}(s)}=\frac{-L_2 s+R_{\mathrm{Load}}(1-D)^2}{R_{\mathrm{Load}}C_{\mathrm{dc}}(1-D)s+2(1-D)} \tag{2}$$

### 4.2 Li-ion battery

The battery pack control can produce a smooth supply of the DC motor current. The second-order cut-off frequency of 50Hz Bessel low-pass filter has been applied to reduce output current ripples or avoid instantaneous large changes.

Assuming the converter is lossless, the DC motor current is equal to the battery current, which can be expressed as:

$$V_{\mathrm{load}}\times I_{\mathrm{load}}=V_{\mathrm{batt}}\times I_{\mathrm{batt}};I_{\mathrm{batt}}=\frac{V_{\mathrm{load}}\times I_{\mathrm{load}}}{V_{\mathrm{batt}}} \tag{3}$$

The reference current of the battery pack is expressed as:

$$I_{\mathrm{batt}}^{*}=\frac{V_{\mathrm{load}}\times I_{\mathrm{load}}}{V_{\mathrm{batt}}}G_{\mathrm{LP}}(s) \tag{4}$$

Where $V_{\mathrm{load}}$ and $I_{\mathrm{load}}$ stand for the voltage and current of DC motor; $V_{\mathrm{bat}}$ and $I_{\mathrm{bat}}$ are the voltage and current of Li-ion battery.

$G_{\mathrm{LP}}(s)$ is the transfer function of Bessel low-pass filter which can be expressed as:

$$G_{\mathrm{LP}}(s)=\frac{\theta_n(0)}{\theta_n(s/\omega_0)}=\frac{b(1)s^n+b(2)s^{n-1}+\cdots+b(n+1)}{s^n+a(2)s^{n-1}+\cdots+a(n+1)} \tag{5}$$

$\theta_n(s)$ is the reverse Bessel polynomials, $\omega_0$ is the cutoff frequency, $a(n)$ and $b(n)$ are coefficient of the Bessel polynomials.

The Bessel filter is a linear filter with the largest flat group delay or linear phase response and can fully retain a filtered waveform and maintain a stable group delay. Once the battery output reference current is established, the converter is controlled by the peak current controller. Fig.4 is a specific control block (where $i_{\mathrm{batt}}^{*}$ and $i_{\mathrm{batt\text{-}sen}}^{*}$ are the per unit of actual and rated battery current; $G_{3,4}$ are the switching signal of $T_3$ and $T_4$).

Moreover, Li-ion battery power dynamic limitation rule-based control based on the SOC of the super capacitor is introduced to avoid the frequent switch of Li-ion batteries (charge and discharge) and reduce the stress on the Li-ion batteries.

The operating modes are as follows:

**Mode1**: When the HESS is charging, if the SOC of super-capacitor exceeds the upper limitation $Q_{\mathrm{sc\_char\_high}}$, the limitation of Li-ion power is increased to $P_{\mathrm{char\_high\_limit}}$;

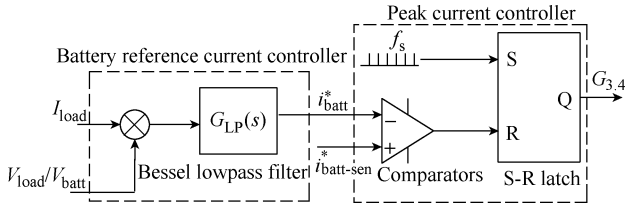


Fig.4 Block diagram of the Li-ion battery pack

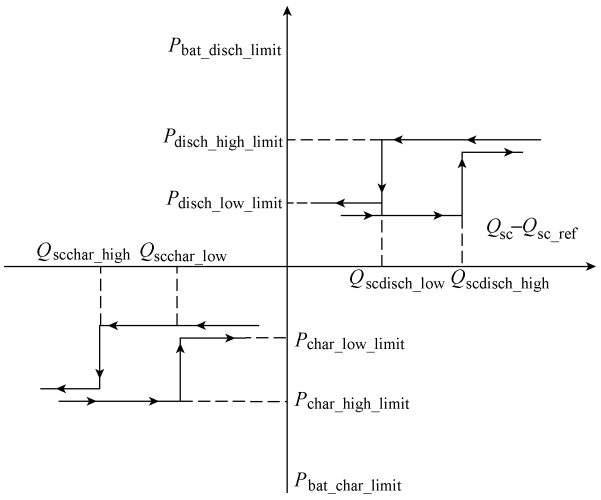


Fig.5 The diagram of Li-ion battery power dynamic limitation

if the SOC of super-capacitor is lower than the lower limitation $Q_{\mathrm{sc\_char\_low}}$, the limitation of Li-ion power is reduced to $P_{\mathrm{char\_low\_limit}}$. The dynamic limitation of the Li-ion battery can be written as:

$$\text{If } Q_{\mathrm{sc}}-Q_{\mathrm{scref}}\geqslant Q_{\mathrm{scchar\_high}},\quad P_{\mathrm{bat\_char\_limit}}=P_{\mathrm{char\_high\_limit}} \tag{6}$$

$$\text{If } Q_{\mathrm{sc}}-Q_{\mathrm{scref}}<Q_{\mathrm{scchar\_low}},\quad P_{\mathrm{bat\_char\_limit}}=P_{\mathrm{char\_high\_limit}} \tag{7}$$

**Mode 2**:When the HESS is discharging, if the SOC of super-capacitor exceeds the upper limitation $Q_{\mathrm{sc\_disch\_high}}$, the limitation of Li-ion power is increased to $P_{\mathrm{disch\_high\_limit}}$; if the SOC of super-capacitor is lower than the lower limitation $Q_{\mathrm{sc\_disch\_low}}$, the limitation of Li-ion power is reduced to $P_{\mathrm{disch\_low\_limit}}$. The dynamic limitation of the Li-ion battery can be written as:

$$\text{If } Q_{\mathrm{sc}}-Q_{\mathrm{scref}}\geqslant Q_{\mathrm{scdisch\_high}},\quad P_{\mathrm{bat\_dischlimit}}=P_{\mathrm{disch\_highlimit}} \tag{8}$$

$$\text{If } Q_{\mathrm{sc}}-Q_{\mathrm{scref}}<Q_{\mathrm{scdisch\_low}},\quad P_{\mathrm{bat\_dischlimit}}=P_{\mathrm{disch\_highlimit}} \tag{9}$$

The above control parameters can be acquired by a hybrid algorithm based on particle swarm optimization and Nelder-Mead simplex approach.

### 4.3 Continuous recharge of super-capacitor from Li-ion battery

In order to ensure enough energy from the super-capacitor, when the SOC of the super-capacitor is below the limit, the super-capacitor charges from the Li-ion battery. Moreover, in the beginning of the driving cycle, a target value of super-capacitor SOC is chosen as the initial value to provide enough energy. An additional control loop based on PI controller, which controls the continuous recharge of super-capacitor from Li-ion battery during the driving phase and also when the electric vehicle is at a standstill, is designed. Fig.6 is a specific block of the additional control loop.

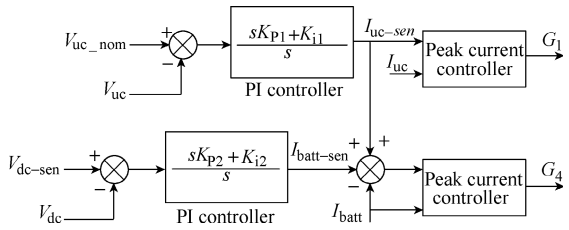


Fig.6 Block diagram of the additional control loop

Where $V_{uc\_nom}$ and $V_{uc}$ are the rated and actual super-capacitor voltage; $I_{uc\text{-}sen}$ and $I_{uc}$ are the rated and actual super-capacitor current; $V_{dc\text{-}sen}$ and $V_{dc}$ are the rated and actual voltage of DC motor; $I_{batt\text{-}sen}$ and $I_{batt}$ are the rated and actual battery current; $G_{1,4}$ are the switching signal of $T_1$ and $T_4$.

### 4.4 Control parameter optimization

The optimization of HESS energy is targeted to solve a mathematical multi-constrained nonlinear problem. It can be described in the following equations:

$$\min_X F(X) = \{f(X)\} \tag{10}$$

Subject to:

$$g_i(X) \leqslant 0, i = 1,2,3,4 \tag{11}$$

$$X_{\min} \leqslant X \leqslant X_{\max} \tag{12}$$

Where is $X = (x_1, x_2, \cdots, x_{10})$ is the control parameter; $x_1$, $x_2$, $x_3$, $x_4$, $x_5$, $x_6$, $x_7$ and $x_8$ represent $P_{disch\_high\_limit}$, $P_{disch\_low\_limit}$, $Q_{sc\_disch\_high}$, $Q_{sc\_disch\_low}$, $P_{char\_high\_limit}$, $P_{char\_low\_limit}$, $Q_{sc\_char\_high}$ and $Q_{sc\_char\_low}$; $x_9$ and $x_{10}$ are PI control parameters to ensure that the energy of super capacitor is kept around its beginning value at the end of each driving cycle ($K_{P1}$ and $T_{i1}$).

In order to reduce the stress of the Li-ion battery pack, the HESS energy management proposed in the paper is designed to reduce the instantaneous power of the Li-ion battery pack under the premise of ensuring the performance of HESS. Therefore, a function aiming at minimizing the battery power RMS of the Li-ion battery is established as shown in Equ.(13).

$$f(X) = \sqrt{\frac{1}{T}\int_0^T P_{Bat}^2(t)\mathrm{d}t} \tag{13}$$

Where $T$ is a time period covering full charging and discharging cycles; $P_{Bat}(t)$ is the instantaneous power of battery charging or discharging.

The hybrid optimization based on particle swarm optimization and Nelder-Mead simplex approach of control parameters is as follows:

(1) Initialize particles and calculate fitness values for each particle. Then find local position($LP$) and assign LP to global position($GP$). $F(LP)=\min\{f_i\}$

(2) Particle swarm optimization: Calculate velocity for each particle and update each particle's position; Then evaluate each particle $f_i=F(X_i)$ and find $LP$, if the $LP$ better than $GP$, assign $LP$ as new $GP$; Otherwise, keep it. When iteration$>m_1$, go to the next step.

(3) Nelder-mead simplex approach: Define verticles $GP$, $LP$, $WP$(worst position $F(WP)=\max\{f_i\}$); Then, reflect, expanse, contract, shrink the vertices; Evaluate each particle $f_i=F(X_i)$; and find $LP$, if the $LP$ better than $GP$, assign $LP$ as new $GP$; Otherwise, keep it. When iteration$>m_2$, end.

Li-ion battery power constraints:

$$E_{Batcons} \leqslant N_{SB}.N_{PB}.C_{celbat}.U_{celbat}.\eta_{DOD} \tag{14}$$

$$P_{Batcons} \leqslant N_{SB}.N_{PB}.C_{celbat}.I_{cel\_bat}^{D} \tag{15}$$

$$P_{Batrec} \leqslant N_{SB}.N_{PB}.C_{celbat}.I_{cel\_bat}^{C} \tag{16}$$

Where $E_{Batcons}$ is HESS energy consumption; $N_{SB}.N_{PB}$ is the Li-ion battery cells; $N_{SB}$ is the number of cells in series and $N_{PB}$ is the number of cells in parallel; $C_{celbat}$、$U_{celbat}$ are respectively the rated capacity and cut-off voltage of Li-ion battery cells; $\eta_{DOD}$ is the discharge depth; $I_{cel\_bat}^{D}$ and $I_{cel\_bat}^{C}$ are respectively the discharging current and charging current of Li-ion battery; $P_{Batcons}$ and $P_{Batrec}$ are respectively the peak lithium battery discharging and charging power;

Super-capacitor power constraints:

$$\Delta E_{sc} \leqslant \frac{3N_{P\_sc}}{8N_{S\_sc}}.C_{celsc}.U_{sc\_max}^2 \tag{17}$$

Where $\Delta E_{sc}$ is the energy requirement of super-capacitor to fulfill the transient powers ($\Delta E_{sc} = E_{sc\_max} - E_{sc\_min}$), $N_{P\_sc}$, $N_{S\_sc}$ are the number of Super-capacitor branches in parallel and in series; $C_{celsc}$, $U_{sc\_max}$ are the rated capacity and maximum peak of the super-capacitor output voltage.

## 5 Simulation and experimental analysis

### 5.1 Simulation of proposed HESS

In the part, a simulation model of the proposed HESS is built on Matlab/Simulink.

**Table 3 The parameters of HESS**

| Parameters | Value |
|---|---|
| $N_{SB}.N_{PB}$ | 185 |
| $N_{P\_sc}.N_{S\_sc}$ | 570 |
| Li-ion battery $\eta_{DOD}$ | 80% |
| Li-ion battery initial SOC | 1 |
| Super-capacitor initial SOC | 0.94 |
| Li-ion battery En/(kW·h), $P_{max}$/W | 10, 200 |
| Super-capacitor En/(kW·h), $P_{max}$/W | 0.25, 200 |

**Table 4 Control parameters of HESS**

| Parameters | Value |
|---|---|
| $P_{disch\_high\_limit}(x_1)$ | $N_{SB}.N_{PB}.C_{celbat}.I_{cel\_bat}^{D}$ |
| $P_{disch\_low\_limit}(x_2)$ | 0 |
| $Q_{sc\_disch\_high}(x_3)$ | 0.81 |
| $Q_{sc\_disch\_low}(x_4)$ | 0.42 |
| $P_{char\_high\_limit}(x_5)$ | $0.05N_{SB}.N_{PB}.C_{celbat}.I_{cel\_bat}^{C}$ |
| $P_{char\_low\_limit}(x_6)$ | 0 |
| $Q_{sc\_char\_high}(x_7)$ | 0.97 |
| $Q_{sc\_char\_low}(x_8)$ | 0.94 |
| $K_{p1}(x_9)$ | 0.08 |
| $T_{i1}(x_{10})$ | 0.02 |

The real-time SOC of Li-ion battery and super-capacitor are as follows:

$$Q_{\text{bat}} = Q_{\text{bat}0} - \frac{\int_0^t p_{\text{bat}}(t)\text{d}t}{E_{n\_\text{sc}}} \tag{18}$$

$$Q_{\text{sc}} = Q_{\text{sc}0} - \frac{\int_0^t p_{\text{sc}}(t)\text{d}t}{E_{n\_\text{sc}}} \tag{19}$$

This paper simulates the proposed HESS dealing with power command with large fluctuations and the simulation waveform is shown in Fig.6.

As can be seen from Fig.7, the response of the proposed HESS is timely when the power command fluctuates violently. From Fig.7(b), it can be seen the Li-ion batteries are responsible for non-high-frequency components and the super-capacitors are responsible for high- frequency components.

The proposed HESS takes full advantage of Li-ion batteries and super-capacitors, so that the super-capacitor maintains the ability of power conditioning and improves the overall performance of HESS.

### 5.2 Simulation and experiment of proposed HESS applied to electric vehicles

#### 5.2.1 Simulation

The simulation model of the proposed HESS applied to a typical car driving cycle is built on Matlab/ Simulink to test the dynamic performance of the system. The parameters of simulation system are presented in Table 5.

The simulation of cars during the acceleration mode, constant speed mode, braking mode and parking charging mode are built on Matlab/Simulink, and the stability of the load side and load side voltage, battery, super capacitor current ripple are observed.

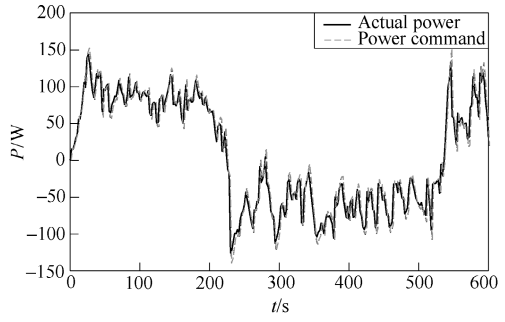


(a) Power command and actual power

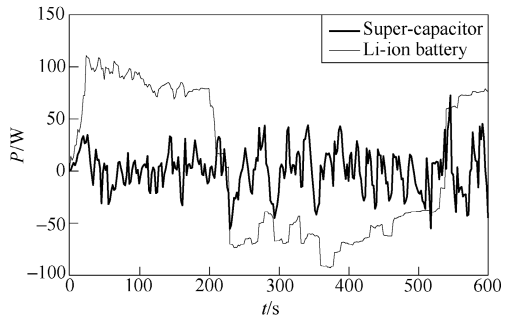


(b) Power of the super-capacitor and Li-ion battery

Fig.7 Simulation results of the proposed HESS

**Table 5 Simulation system specification**

| Detailed simulation parameters | |
|---|---|
| DC side voltage/V | $V_{\text{DC-nom}}$ =300 |
| Rated voltage of the battery pack/V | $V_{\text{batt-nom}}$ =144 |
| $C_{\text{DC}}$/μF | 4400 |
| Rated voltage of the super capacitor/V | $V_{\text{UC-nom}}$ =125 |
| $L_1$/mH | 10.12 |
| $L_2$/μH | 580 |
| $M$/μH | 580 |
| Switching frequency/kHz | $f_s$ =15 |
| Sampling time/μs | $T_{\text{st}}$ =5 |

As shown in Fig.8, the load current corresponding to a conventional driving cycle, the load current is very smooth, (added to the battery group simulation analysis), almost no ripple.

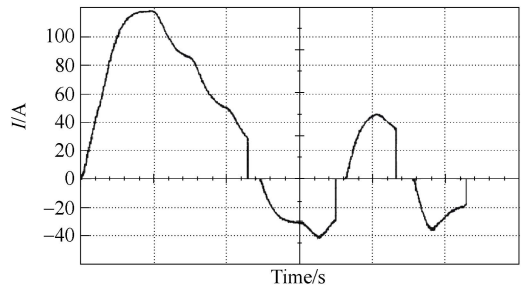


(a) Battery current

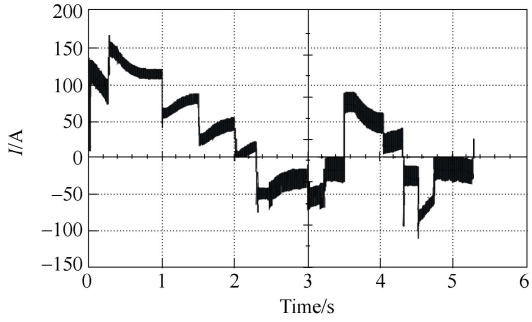


(b) Super-capacitor current

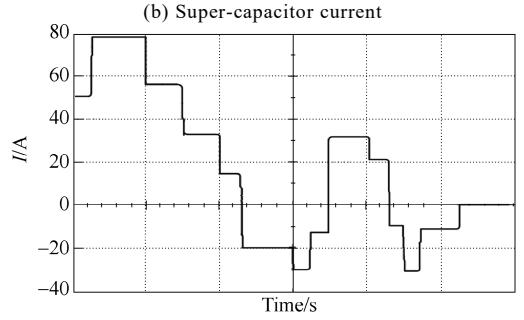


(c) Load current

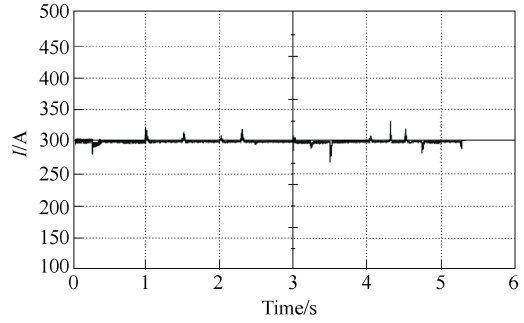


(d) Load voltage

Fig.8 Simulation results of the proposed HESS applied on electric vehicles

Compared to the super-capacitor current, the battery current changes are smoother with no instantaneous perturbations. The output current of the battery pack is smooth and has minimal ripple content, which extends the life of the battery pack and can reduce the loss due to current ripple caused by the DC motor. The super-capacitors are responsible for the high-frequency contents of the load, so a sudden change in its current is normal. At the same time, we can see that a small amount of fluctuation in the load voltage, which is caused by vehicle acceleration or braking, and the voltage can be quickly restored to 300V by the super-capacitor.

### 5.2.2 Experiment

Finally, the paper makes an experiment to observe changes of the current of batteries and super-capacitors with step changes in the load. In order to fulfill the conditions in a laboratory environment, we built a small scale experiment and adopted boostcap PC2500 super-capacitor, which switches are HGTG30N60A4D IGBT, and the voltage and current senor are respectively LV 20-P and LA100-P. TMS320F2812 DSP is selected as a feedback and control systems. The values of inductors $L_1$, $L_2$, and M were 2mH, 50μH, 50μH. The actual values of these devices are shown in Table 6.

Fig.9 shows the excellent ability of the proposed HESS in response to the acceleration and braking condition of electric cars. For energy storage systems with super-capacitors, when $t=3$ and the load step ups, the battery current is smooth and doing a slow controlled ramop, meanwhile, the super-capacitor repeatedly high-current discharge and DC voltage is stabilized at 20V which the overall volatility is less than 5%; When $t=7$ the load set down, super-capacitor recovered the braking energy, as we can see, the super-capacitor current is negative. For energy storage system without super-capacitors, the battery pack as a single storage is responsible for the set change in the load and has high fluctuation and ripple in current, which will reduce the life of battery. Compared with the proposed HESS, it is not suitable for electric vehicles.

## 6 Conclusions

In this paper, a new hybrid energy storage system for electric vehicles is designed based on a Li-ion battery power dynamic limitation rule-based HESS energy management and a new bi-directional DC/DC converter. The system is compared to traditional hybrid energy storage system, showing it has significant advantage of reduced volume and weight. Moreover, the ripple of output current is reduced and the life of battery is improved.

**Table 6 Experimental equipment and circuit parameters**

| Experimental data | |
|---|---|
| DC side voltage/V | $V_{dc}=20$ |
| Battery/V | $V_{batt}=12$<br>the initial charge state 80% lead-acid battery |
| Super Capacitor | 6 Maxwell Boostcap PC2500 series connection<br>450F, the initial state of charge 12V |
| Switching frequency/kHz | $f_s=20$ |
| Sampling time/μs | $T_{st}=20$ |
| DSP model | TI-TMS320F2812 |
| $L_1$, $L_2$/μH | 1.938 mH, 54.5687 |
| $M$/μH | 52.7866 |
| Switch model | HGTG 30 N 60 A 4 D IGBT |
| Voltage sensor | *LV* 20-*P* |
| Current sensor | *LA* 100-*P* |

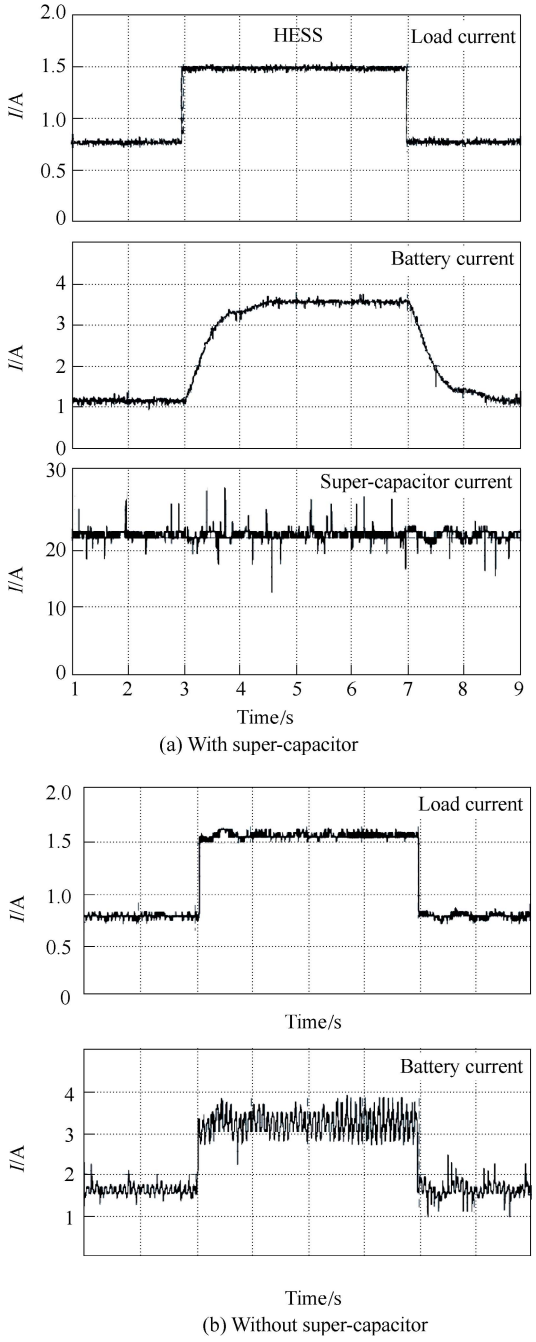


Fig.9 Experiment results of the proposed HESS applied on electric vehicles

## References

[1] Zhikang Shuai, Chao Shen, Xin Yin, Xuan Liu, John Shen, "Fault analysis of inverter-interfaced distributed generators with different control schemes," *IEEE Transactions on Power Delivery*, DOI: 10. 1109/TPWRD. 2017. 2717388.

[2] Zhikang Shuai, Yingyun Sun, Z. John Shen, Wei Tian, Chunming Tu, Yan Li, Xin Yin, "Microgrid stability: classification and a review," *Renewable and Sustainable Energy Reviews*, vol.58, pp. 167-179, Feb. 2016.

[3] N. R. Tummuru, M. K. Mishra, and S. Srinivas, "Dynamic energy management of renewable grid integrated hybrid

energy storage system, " *IEEE Trans. Ind. Electron*., vol. 62, no. 12, pp. 7728-7737, Dec. 2015.
[4] T. Mesbahi, N. Rizoug, F. Khenfri, P. Bartholomeus, and P. Le Moigne, "Dynamical modelling and emulation of Li-ion batteries- supercapacitors hybrid power supply for electric vehicle applications, " *IET Electr. Syst. Transp*., vol.7, no.2, pp. 161-169, Nov. 2016.
[5] A. Santucci, A. Sorniotti, and C. Lekakou, "Power split strategies for hybrid energy storage systems for vehicular applications, " *J. Power Sources*, vol. 258, no.14, pp. 395-407, 2014.
[6] J. Shen, S. Dusmez, and A. Khaligh, "Optimization of sizing and battery cycle life in battery/ultracapacitor hybrid energy storage systems for electric vehicle applications," *IEEE Trans. Ind. Informat*., vol. 10, no. 4, pp. 2112-2121, Nov. 2014.
[7] M. Ecker, J. B. Gerschler, J. Vogel, S. Käbitz, and F. Hust, "Development of a lifetime prediction model for lithiumion batteries based on extended accelerated aging test data," *J. Power Sources*, vol. 215, no.5, pp. 248-257, Oct. 2012.
[8] R. Sadoun, N. Rizoug, P. Bartholomeus, B. Barbedette, and P. Le Moigne, "Optimal sizing of hybrid supply for electric vehicle using Li-ion batteryand supercapacitor," In *Proc. IEEE Veh. Power Propulsion Conf*., pp. 1-8, 2011.
[9] D. Liu, and H. Li, "A ZVS bi-directional DC-DC converter for multiple energy storage elements," *Transactions on Power Electronics*, vol.21, no.5, pp.1513-1517, 2006.
[10] N. M. L. Tan, T. Abe,and H. Akagi, "Design and performance of a bidirectional isolated DC-DC converter for a battery energy storage system,"*IEEE Transactions on Power Electronics*, vol.27, no.3, pp.1237-1248, 2012.
[11] S. Cuk, R. D. Middlebrook,"A new optimum to pology switching DC-to-DC converter," In: *Proceedings of 8th IEEE Power Electronics Specialists Conference*, pp.160-179, 1977.
[12] S. Cuk, "A new zero-ripple switching DC-to-DC converter and integrated magnetics," *IEEE Transactions on Magnetics*, vol.19, no.2, pp.57-75, 1983.
[13] Wuhua Li,Xiangning He, Jianyong Wu, "Isolated interleaved DC/DC converters with winding-cross-coupled inductors," *Transactions of China Electrotechnical Society*, vol.24, no.9, pp.99-106, 2009.
[14] M. E. Choi, S. W. Kim, and S. W. Seo, "Energy management optimization in a battery/supercapacitor Hybrid energy storage system, " *IEEE Trans. Smart Grid*, vol. 3, no. 1, pp. 463-472, Mar. 2012.
[15] Z. Yu, D. Zinger, and A. Bose, "An innovative optimal power allocation strategy for fuel cell, battery and supercapacitor hybrid electric vehicle, "*J. Power Sources*, vol. 196, no. 4, pp. 2351-2359, Feb. 2011.
[16] Zhikang Shuai, Yang Hu, Yelun Peng, Chunming Tu, Z. John Shen, "Dynamic stability analysis of synchronverter-dominated microgrid based on bifurcation theory, " *IEEE Transactions on Industrial Electronics*, vol. 64, no. 9, pp. 7467-7477, Sep. 2017.
[17] Q. Li, W. Chen, Y. Li, S. Liu, and J. Huang, "Energy management strategy for fuel cell/battery/ultracapacitor hybrid vehicle based on fuzzy logic, "*Int. J. Electr. Power Energy Syst*., vol. 43, no. 1, pp. 514-525, Dec. 2012.
[18] Zhikang Shuai, Wen Huang, Chao Shen, Jun Ge, and Z. John Shen, "Characteristics and restraining method of fast transient inrush fault currents in synchronverters," *IEEE Transactions on Industrial Electronics*, vol. 64, no. 9, pp. 7487-7497, Sep. 2017.
[19] A. Castaings, W. Lhomme, R. Trigui, and A. Bouscayrol, "Comparison of energy management strategies of a battery/ supercapacitors system for electric vehicle under real-time constraints, " *Appl. Energy*, vol. 163, pp. 190-200, 2016.
[20] S. K. Kollimalla, M. K. Mishra, and N. L. Narasamma, "Design and analysis of novel control strategy for battery and supercapacitor storage system,"*IEEE Trans. Sustain. Energy*, vol. 5, no. 4, pp. 1137-1144, Oct. 2014.

**Xiangyang Xia** received the B.Sc. and M.Sc. degrees from Central South University, China, in 1991 and 2004, majored in electrical engineering and control engineering, respectively, and the Ph.D. degree from Hunan University, China, in 2009, majored in electrical engineering. Currently, he is a professor in Changsha University of Science and Technology. His research is on the application of electronic technology in power system.

**Xinxin Zhao** received the B.Sc.. degrees from Changsha University of Science and Technology, China, in 2016, majored in electrical engineering. Currently, he is a master student in Changsha University of Science and Technology. His research is on the application of electronic technology in power system.

**Heqing Zeng** received the B.Sc.. degrees from Changsha University of Science and Technology, China, in 2013, majored in electrical engineering. Currently, he is a master student in Changsha University of Science and Technology. His research is on the application of electronic technology in power system.

**Xiaoyong Zeng** received the B.Sc. and M.Sc. degrees from Changsha University of Science and Technology and Wuhan University, China, in 2003 and 2006, majored in electrical engineering and power and machinery. Currently, he is a doctor in Central South University. His research is on the application of electronic technology in power system.